



Treatment of wastewater contaminated with dyes using modified low-cost adsorbents

Ahmed Hassoon Ali

*College of Engineering, Department of Environmental Engineering, Mustansiriyah University, Iraq,
email: env.eng.dr.ahmed@uomustansiriyah.edu.iq*

Received 16 June 2018; Accepted 21 November 2018

ABSTRACT

The present study was designed to investigate the removal of three reactive dyes: Reactive Blue (RB), Reactive Red (RR) and Reactive Yellow (RY) from simulated textile wastewater in single and mixed (ternary) systems using adsorption process. Modified low-cost adsorbents: rice husk (RH), saw dust (SD) and sewage sludge (SS) in addition to granular activated carbon were used as adsorbents. RH was found to have a high removal efficiency. Batch experiments were achieved to study the effects of pH, dosage, contact time and initial concentration onto adsorption process using RH. The optimum conditions were found to be 2, 3 g, 150 min and 50 mg/L, respectively. The maximum removal efficiency was 95.77%, 89.26% and 80.36% for RB, RR and RY, respectively, for single system. Adsorption isotherms and kinetic models had been used to fit the experimental data. From which Langmuir and pseudo-second-order models were found to be having high correlation coefficient for the three dyes.

Keywords: Reactive dyes; Adsorption; Rice husk; Saw dust; Sewage sludge; Granular activated carbon

1. Introduction

Wastewater from textile industry can contain a variety of polluting substances including dyes. The increased number of textile industries has shown a significant increase in the use of synthetic complex organic dyes as the coloring materials. Color is the first contamination to be recognized in the wastewater and has to be removed before discharging into water bodies or on land. The presence of very small amount of dyes in water (less than 1 ppm for some dyes) is highly visible and affects the aesthetic merit, water transparency and gas solubility in lakes, river and other water bodies. The removal of color from water is often more important than the removal of the soluble colorless organic substance, which usually contribute the major fraction of the biochemical oxygen demand (BOD). Dyes, however, are more difficult to treat because of their synthetic origin and mainly complex aromatic molecular structures [1].

Adsorption is a physical–chemical technique that involves mass-transfer from liquid to solid-phase to remove or at least reduce chemical residues in wastewater [2].

Two-dimensional (2D) carbon nanomaterials generally display some limitations in adsorption applications due to easy agglomeration. This problem was solved, as-synthesized sandwiched nanocomposites made of Fe_3O_4 nanoparticles, different materials such as poly(allylamine) hydrochloride molecules and carboxylate graphene oxide sheets prepared using a layer-by-layer (LbL) self-assembly method. The successfully synthesized sandwiched structures nanocomposites have outstanding organic dye adsorption performance, stability and recycling [3]. Activated carbon is most widely used as an adsorbent in treatment of wastewater. Despite of its efficiency in adsorption process, this adsorbent has a high-cost which makes it no longer attractive to be used in small-scale industries; because of this problem, recent years researches have to produce other alternative low-cost adsorbents that can substitute activated carbon in wastewater treatment. This type of low-cost adsorbents derives from agriculture waste; industrial by-products or natural materials [4]. In this work, the removal efficiency of three dyes (Reactive Blue [RB], Reactive Red [RR] and Reactive Yellow

[RY]) was investigated using low-cost adsorbents obtained from plant wastes and sewage sludge as a replacement for costly conventional methods using commercial granular activated carbon. Batch studies were used to evaluate the influence of various experimental parameters including pH, adsorbent dosage, contact time and initial concentration of adsorbate onto removal efficiency using best adsorbent in single and mixed (ternary) system. Various adsorption isotherm and kinetic models were applied to fit the experimental data. Prediction of removal efficiency for adsorption process was carried out using multiple correlation equations.

2. Materials and methods

2.1. Reactive dyes

Three dyes (Reactive Blue [RB], Reactive Red [RR] and Reactive Yellow [RY]) had been supplied from AL-Kut textile Factory south of Baghdad (Department of Dyeing and Printing). Simulated stock solutions of 1,000 mg/L had been prepared by dissolving 1 g of each dye in 1 L distilled water then diluted to the desired solution concentration of single dyes (RB, RR and RY) and ternary system (BRY). Table 1 shows specifications of these dyes. Some suppliers consider these specifications as know-how due to commercial reasons [5–8].

2.2. Type of adsorbent

Three types of nonconventional adsorbents were prepared: rice husk (RH), sewage sludge (SS) and saw dust (SD) in addition to commercial granular activated carbon (GAC). The direct use of the raw wastes as adsorbents had been found to be limited due to leaching of organic substances such as lignin, tannin, pectin and cellulose into the solution [9]. To resolve these problems, chemical modification had been used as a technique to improve their physical, chemical properties and adsorption capacity [10,11].

2.3. Properties of prepared adsorbents

The GAC, RH, SS and SD samples were sieved into mesh 0.6, 1 mm by using standard sieves. For non-spherical

particles, the particle diameter is defined as an equivalent diameter of a spherical particle with the same volume. As an approximation, the particle diameter was calculated from the geometric mean of the two consecutive sieve openings without introducing serious errors. The geometric mean diameter is given by, $d_{gm} = (d_1 d_2)^{1/2}$, where d_1 is the diameter of the lower sieve on which the particles are retained and d_2 is the diameter of the upper sieve through which the particles pass [12]. The physical, chemical properties and cost of purchasing/preparation of adsorbents were carried out at Catalysts Department in the Center of Petroleum Research and Development (Ministry of oil/Iraq) as listed in Table 2.

2.4. Analytical techniques of dyes concentrations measurement

There are a number of analytical methods that may be used for quantitative analysis of dyes solution such as: first, chemical oxygen demand (COD) to characterize the content of organics which can be oxidized to inorganic. Second, UV-visible absorption spectrophotometer method [13–15].

UV-visible absorption spectrophotometer method is the common procedure in determination of colorant concentration in their mixture. The main principle in quantitative UV-visible spectrophotometer technique is linear relation between absorbance A and concentration of dissolved sample C (mg/L) which is given by Beer–Lambert law Eq. (1) [15–17].

$$A = K C + E \quad (1)$$

where A is absorbance of light at wavelength; K is absorbance coefficient (slope of linear relation); C is concentration of dye in solution (mg/L); E is intercept of linear relation.

For multi-components solution the absorptive (absorbance coefficient for each dye is determined from absorbance measurement of dye at specific dye concentration when absorbance linear relation is constructed by plotting absorbance of each single dye against dye concentration at its wavelength and re-plot at wavelengths of other dyes in the mixture of dye solution. These determined coefficients

Table 1
Main characteristics of reactive dyes

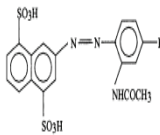
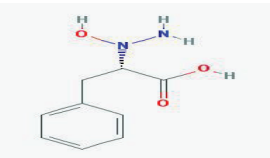
Item	Reactive blue (RB)	Reactive Red (RR)	Reactive Yellow (RY)
Trade name	Cibacron Blue FNR	Cibacron Red FN-R	Cibacron Yellow FN-2R
Origin	Swiss	Swiss	Swiss
Phase	Solid/powder package 25 kg	Solid/powder package 25 kg	Solid/powder package 25 kg
Wavelength (nm)	690	540	501
Molecular formula	$C_{29}H_{23}CuFN_9O_{12}S_3.3Na$	$C_{29}H_{15}ClFN_7O_{13}S_4Na_4$	$C_9H_{12}N_2O_3$
pH	5.5–6	5.5–6	5.5–6
Molecular weight g/mol	936.45	944.2	196
Chemical structure		Not disclosed by the manufacturer	

Table 2
Adsorbents specifications

Specifications	Adsorbents			
	GAC	RH	SS	SD
Source	Uncarbo company Italy form local markets	Local Iraqi mills	AL-Rustomya treatment unit	Collected from a local furniture factory
Origin	Coconut shell	Rice milling waste	Drying bed after primary settling	Sawmill waste
Bulk density* (real density) (kg/m ³)	641 (1,544)	233.52 (1,390)	612.75 (2,500)	462.05 (1,509)
Surface area (m ² /g)	351.965	136.69	35.072	10.1712
Porosity% ϵ	53.44	83.2	75.49	69.38
Pore volume (cm ³ /g)	0.422	0.054	0.544	Nil
CEC (meq/100 g)	58.315	116.8	83.380	43.118
Cost of preparation/purchase \$/Kg	1,600	25	38	28
	Purchased	Prepared	Prepared	Prepared

* Bulk density = (1- porosity) \times real density.

are then used to determine the value of unknown dye concentration by using Eq. (2) which can be solved simultaneously by forming matrix which is called multiple linear regression analysis [18,19].

$$\begin{bmatrix} A_1 \\ A_2 \\ \vdots \\ A_n \end{bmatrix} = \begin{bmatrix} K_{11} & K_{12} & \dots & K_{1m} \\ K_{21} & K_{22} & \dots & K_{2m} \\ \vdots & \vdots & \dots & \vdots \\ K_{n1} & K_{n2} & \dots & K_{nm} \end{bmatrix} \begin{bmatrix} C_1 \\ C_2 \\ \vdots \\ C_m \end{bmatrix} + \begin{bmatrix} E_1 \\ E_2 \\ \vdots \\ E_n \end{bmatrix} \quad (2)$$

where A_i is the absorbance at λ_i wavelength. K_{ij} is absorbance coefficient of component (i) at wavelength of component (j). C_j is concentration of j th component; E_i is error of measurement (intercept value of linear relation) which can be ignored.

2.5. Analytical methods (calibration curves for analyses of single and multi-dyes)

Seven solution of single dyes (RB, RR and RY) with concentration (5, 10, 25, 50, 75, 100 and 150 mg/L) were prepared from the serial dilution of stock solution. Absorbance at its wavelengths (609, 540 and 501 nm) for RB, RR and RY, respectively, were measured. Then, the linear relation was plotted between absorbance and each dye concentration at each wavelength (λ) and the process was repeated for each dyes, respectively, in order to get absorbance coefficients to estimate the concentration of unknown dyes.

2.6. Adsorption and kinetics experiments

At first, the adsorption experiments were carried out to select the best adsorbent for dyes removal as a function of pH. Then, the effect of various parameters including dosage, contact time and initial concentration on the removal efficiency of RB, RR and RY using best adsorbent have been determined. All the experiments had been done at room temperature (25°C \pm 5°C). Samples for measurement of

dyes concentration were withdrawn using a pipette from a height of 2–3 cm below the surface in each jar (1 L capacity). Percentage of dye removal was calculated by Eq. (3):

$$\text{Removal (\%)} = \frac{C_r - C_t}{C_r} \times 100 \quad (3)$$

where C_r and C_t are the concentration in raw and treated solutions, respectively.

The efficiency of removing RB, RR and RY mixtures (ternary system) using best adsorbent was investigated using dyes mixture ratio of 1:1:1, where the initial concentration is 50 mg/L and pH, dosage and contact time are fixed at optimum values obtained from studying the effect of each parameters as will be discussed later. The concentration of each dye at different time was determined from the calibration curve plotted between absorbance and concentration of the three dyes as explained in section 2.4 and shown in Fig. 1. Then, the removal efficiency was calculated using Eq. (3).

The kinetic parameters for the adsorption process were studied by varying contact time from 15 to 180 min. pH, adsorbents dosages and initial concentration were fixed at optimum values obtained from adsorption experiments as will cleared later. Volume of samples was fixed at 100 mL. At the desired time interval (15, 30, 45, 60, 90, 120, 180 min) the samples were analyzed to determine the amount of adsorbed ion per mass of adsorbent (q_t , mg/g) at time (t) using Eq. (4):

$$q_t = \frac{(C_o - C_t)}{m} V \quad (4)$$

where C_o is the dye initial concentration (mg/L), C_t is the concentration of dye (mg/L) at time (t), V is the volume of sample 100 mL and m is the mass of adsorbent (g). q_t vs. t was plotted to find the model to fit the experimental data (pseudo-first-order, pseudo-second-order and intra-particle diffusion models).

3. Results and discussion

3.1. Selection of the best adsorbent

To select the best adsorbent from GAC, RH, SS and SD, pH of dyes solution was varied in the range (2, 4, 6, 8, 10 and 12) while the adsorbent dosages and initial concentration are fixed at 1 g and 50 mg/L, respectively. The results are shown in Figs. 2–4. From these figures, it can be seen that the dyes removal efficiency by RH is greater than those by other adsorbents. The arrangements of adsorbents as a function of dye removal efficiency are as follows:

RH > SS > GAC > SD

This behavior of RH adsorbent may be attributed to the cation exchange capacity, as shown in Table 2 for RH (116.8 meq/100 g) > SS (83.380) > GAC (58.315 meq/100 g) > SD (43.118 meq/100 g). The RB, RR and RY play an anionic species in their solutions, due to the decreasing in pH of distilled water from 6.5 to 6 during preparation of solutions. Also, the results showed that as the pH increased the removal efficiency decreased. At acidic pH, the positively charged species start dominating and the surface tends to acquire a positive charge, while the adsorbate (dyes) species are still negatively charged. As the adsorbent surface is positively charged the increasing electrostatic attraction between negatively charged adsorbate species and positively charged adsorbent particles would lead to increased adsorption of reactive dyes [20]. This can be explained on the basis that positively charged surface is formed on the adsorbents at lower pH due to adsorption of hydrogen ions on the surface of adsorbents. The decrease in the amount of dye adsorbed on surface of the

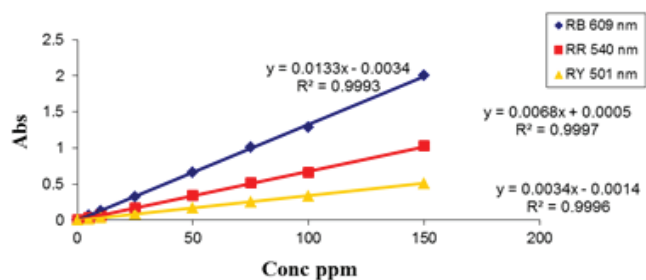


Fig. 1. Calibration curve for the three dyes at different wavelength.

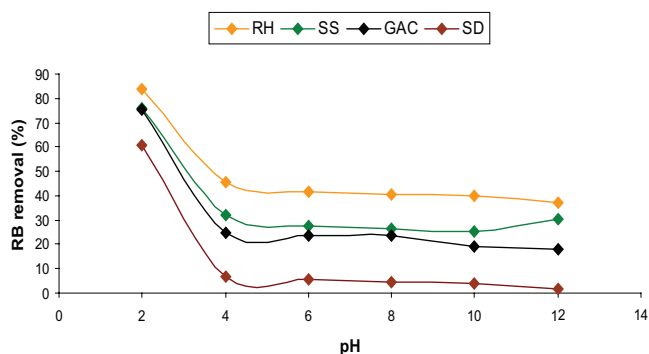


Fig. 2. RB removal as a function of pH at adsorbent dose = 1 g, initial concentration = 50 mg/L.

adsorbents with increase in pH is in good agreement with the data reported earlier [21]. Thus the maximum removal efficiency decreased (from 83.994% to 36.958%, from 70.176% to 24.65% and from 48.241% to 10.026% for RB, RR and RY, respectively) as the pH increases (from 2 to 12).

Thus, RH will be used in further experiments to determine the effects of different parameters on its adsorption capacity for removing reactive dyes in single and mixed system.

3.2. Factors affecting RH performance

3.2.1. Effect of pH

The best pH for the removal of all dyes using RH as found in pervious experiment was 2. Thus the pH of the three reactive dyes solution was adjusted to this value in the next experiments.

3.2.2. Effect of contact time

The effect of contact times onto dye removal efficiency are shown in Fig. 5. The pH, dosages and initial concentration are kept constant at 2, 1 g and 50 mg/L, respectively.

Dye removal was rapid at initial stage (about 90 min) with removal efficiency is 81.834%, 65.985% and 45.231% for RB, RR and RY, respectively) but decreased with the increase of time. Initially rapid increase was due to the presence of large number of vacant site and with the passage of time, number of active sites decreased which were responsible for the reduction of adsorption rate [22]. The optimum contact time was observed to be 150 min for all the dyes with maximum

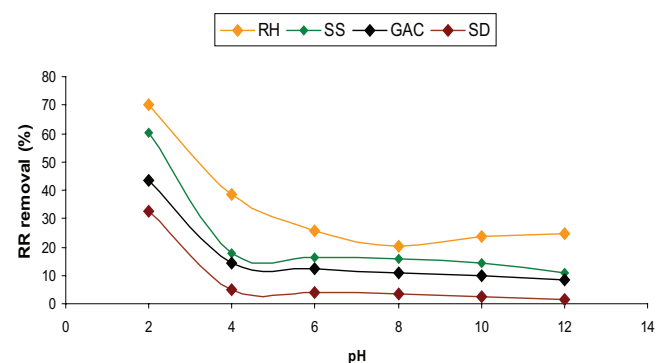


Fig. 3. RR removal as a function of pH at adsorbent dose = 1 g, initial concentration = 50 mg/L.

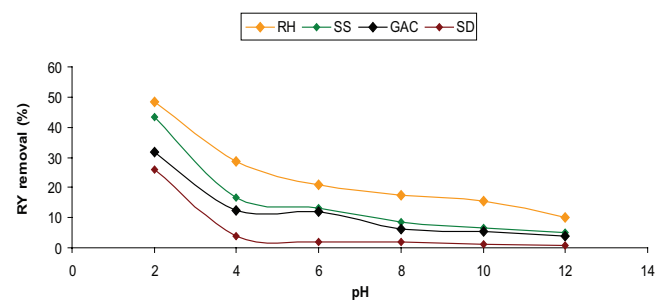


Fig. 4. RY removal as a function of pH at adsorbent dose = 1 g, initial concentration = 50 mg/L.

removal efficiency of 84.14%, 71.32% and 53.21% for RB, RR and RY, respectively.

3.2.3. Effect of RH dosage

For optimizing the amount of adsorbents, experiments were performed using best pH and contact time obtained from previous experiments and 50 mg/L initial dye concentration and was shaken for 150 min after adding different amount of adsorbents (0.5–4.0 g). The results are shown in Fig. 6. It was observed that adsorption of dye increased with the increase of the amount of adsorbents and then attained constant value at equilibrium. The optimum amount was found to be 3.0 g which was used for all subsequent adsorption experiments. The removal efficiency at this dose is 95.77%, 89.26% and 80.36% for RB, RR and RY, respectively. It is readily understood that the number of available adsorption sites increases by increasing the adsorbent dosage and this, therefore, results in an increase in the percentage of dye adsorbed. The decrease in adsorption efficiency with an increase in the adsorbent dosage is mainly because of the unsaturation of adsorption sites through the adsorption process [20,23]. Another reason may be the inter-particle interaction, such as aggregation, resulting from high adsorbent dosage. Such aggregation would lead to a decrease in the total surface area of the adsorbent and on an increase in diffusional path length [20].

3.2.4. Effect of initial concentration

The effect of the initial concentration of the RB, RR and RY dyes on removal efficiency was investigated at a

different concentration range of 5–150 mg/L on RH under previously determined optimum conditions. The maximum removal is 95.77%, 89.26% and 80.36% for RB, RR and RY, respectively, which is obtained at initial concentration of 50 mg/L. According to the results in Fig. 7, it shows that as the initial concentration increases up to 50 mg/L, the dye removal efficiency increases; since at low ratio of adsorbate/adsorbent (i.e., dye/RH) there are more adsorption sites available for dye removal. As the concentration increased beyond 50 mg/L, the ratio increased and consequently the adsorption sites become insufficient to adsorb all dyes molecules [24].

3.3. Treatment of mixed dye solutions using RH

The efficiency of removing RB, RR and RY mixtures (ternary system) using RH was investigated. The ratio of dyes mixture was 1:1:1, where the initial concentration and pH are fixed at 50 mg/L and 2, respectively. As shown in Fig. 8, the maximum removal efficiency is 93.576%, 82.916% and 73.358% for RB, RR and RY, respectively. Maximum removal efficiency for mixed dyes is obtained at 3 g then became constant. However, in single dyes system, the maximum removal efficiency is obtained 3 g and it is still higher than that for mixed system which is due to competition between dyes toward RH. The less dye solubility, the higher removal efficiency [25]. Hence the maximum removal efficiency in mixed system is less by 2.291%, 7.107% and 8.713% in compared with single system for RB, RR and RY dyes, respectively.

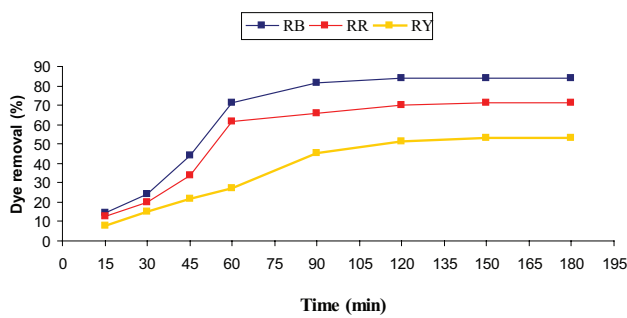


Fig. 5. Effect of contact time of RH on the removal efficiency of RB, RR and RY.

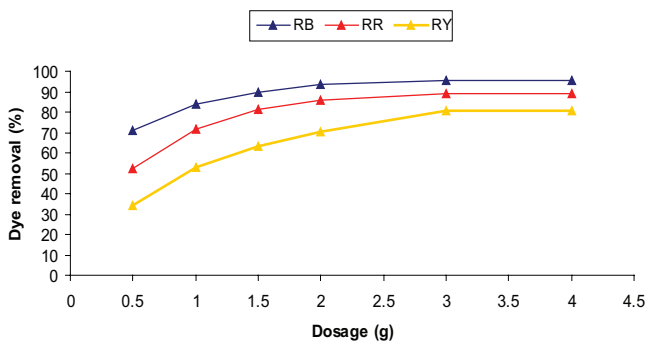


Fig. 6. Effect of RH dosage on the removal efficiency of RB, RR and RY.

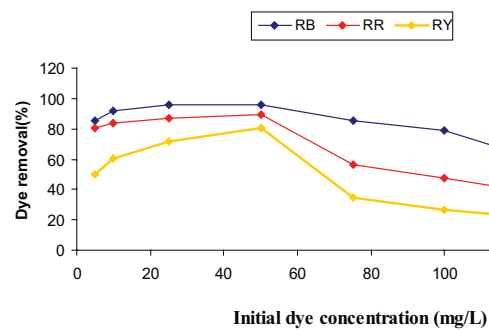


Fig. 7. Effect of initial concentration on the removal efficiency of RB, RR and RY.

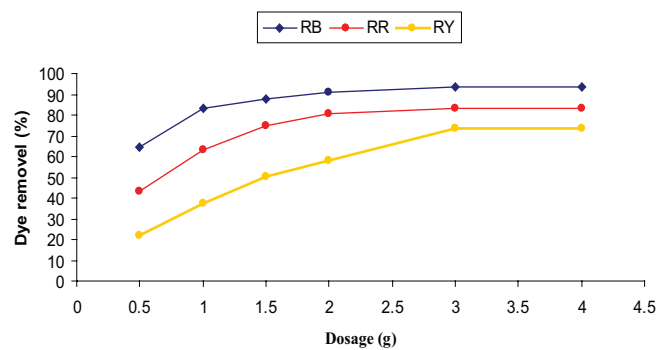


Fig. 8. Effect of RH dosage on the removal efficiency of RB, RR and RY in ternary system.

3.4. Multiple correlations for adsorption process

The removal efficiency of reactive dyes by RH in batch system is affected by many factors including pH, contact time (min), dosage (g) and initial concentration (mg/L). The degree of relationship existing between the dyes removal and these factors are found to be simulated with the regression equation by the application of Excel program. The dye removal efficiency has an optimum value for each factor. The optimum value for each factor was found and put in the following equation: $y = aX_1^b X_2^c X_3^d X_4^e X_5^f$ to calculate the correlation coefficient. The best represented equations for dyes removal and correlation coefficients are shown in Table 3.

3.5. Adsorption isotherm constants for dyes onto RH

3.5.1. Single-component system

The adsorption isotherm for single-component systems of RB, RR and RY, respectively, onto RH are shown in Figs. 9–12

Table 3
Best equation of RH dye removal and its correlation coefficient for RB, RR and RY

Dye	R ²	Equation	y _{practical}	y _{theoretical}
RB	91.581	$y = 5.66 \frac{x_2^{0.692}}{x_1^{0.436} x_3^{0.041} x_4^{0.1098}}$	95.960	90.026
RR	90.266	$y = 10.31 \frac{x_2^{0.676}}{x_1^{0.633} x_3^{0.044} x_4^{0.210}}$	89.260	82.408
RY	91.319	$y = 7.65 \frac{x_2^{0.753}}{x_1^{0.766} x_3^{0.026} x_4^{0.238}}$	80.360	74.974

where y: dye removal efficiency (%), X₁: pH, X₂: contact time (min), X₃: dosage adsorbent (mg), X₄: initial concentration (mg/L), y_{practical}: dye removal efficiency (%) calculated from batch tests by using Eq. (3) and y_{theoretical}: dye removal efficiency (%) calculated from the equation by multiple correlation.

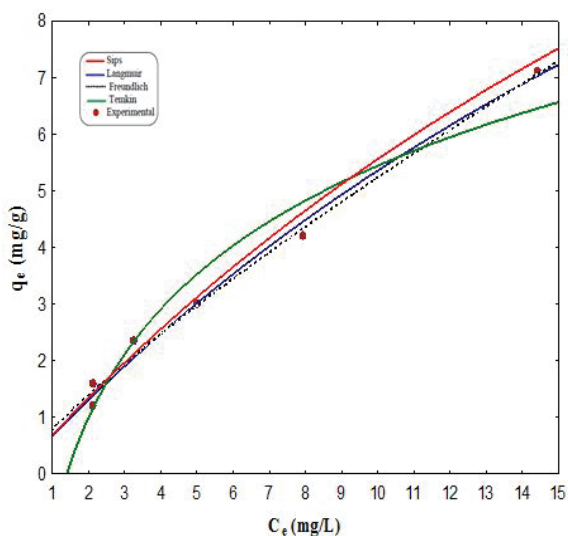


Fig. 9. Adsorption isotherm for single RB onto RH.

using four models Freundlich, Langmuir, Temkin and combination of Langmuir–Freundlich as listed in Table 4 whereas Fig. 11 shows a comparison between dyes adsorption capacity using Langmuir model. The parameters for each model obtained from non-linear statistical fit of the equations to the

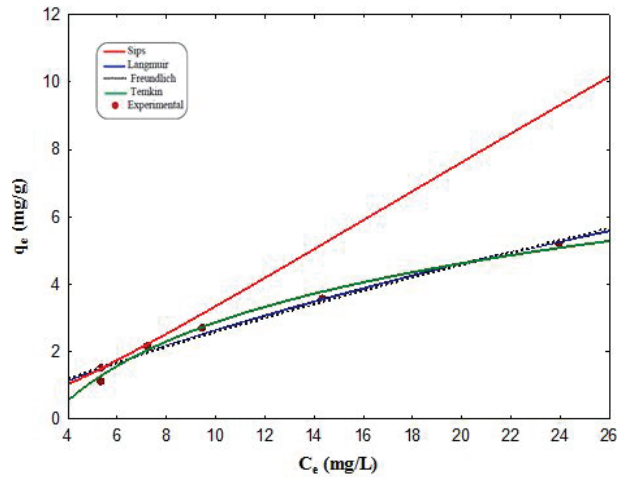


Fig. 10. Adsorption isotherm for single RR onto RH.

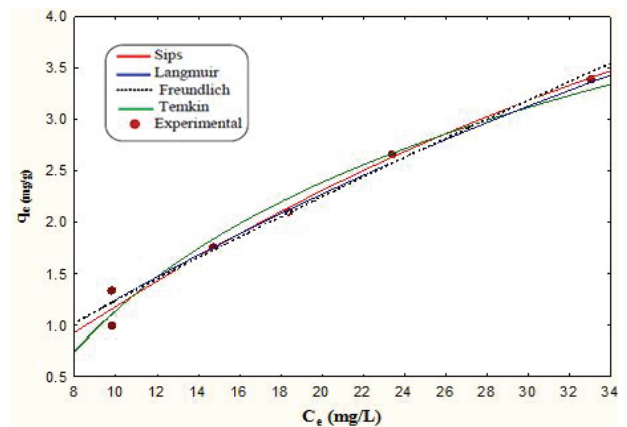


Fig. 11. Adsorption isotherm for single RY onto RH.

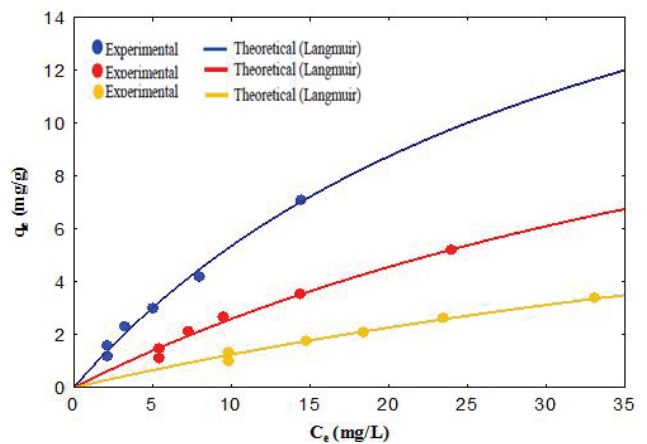


Fig. 12. RH adsorption isotherm in single system for RB, RR and RY using Langmuir model.

experimental data (Statistica v6). Table 4 shows parameters of single-solute isotherm for RB, RR and RY uptake onto RH.

From the above figures and Table 4 for single-component systems, one can conclude the following:

- The equilibrium isotherm for each solute is of favorable type since $R_L < 1$ ($R_L = 0.408, 0.556$ and 0.645 for RB, RR and RY, respectively).
- For RB and RY; Langmuir and Freundlich models gave the best fit of the experimental data with high correlation coefficients (0.996 and 0.990, respectively). While the experimental data for RR were described successfully with Langmuir and Temkin models with correlation coefficient of 0.993.
- Using Langmuir model; it was found that the maximum amount of adsorbate adsorbed per mass of RH (q_m) for RB is greater than that for RR and RY ($q_{m, RB} = 23.895$ mg/g; $q_{m, RR} = 18.844$ mg/g and $q_{m, RY} = 12.614$ mg/g). This may be attributed to that solubility of RB which is less than for

RR and RY. At the same time, the molecular weight for RR is greater than that for RY. The solubility and molecular weight of reactive dyes are listed in Table 3.

- From Temkin, the values of free energy noted as b_1 are 6.360, 5.831 and 4.137 kJ/mole for RB, RR and RY, respectively, which is less than 40 kJ/mole. This confirms that adsorption process of RB, RR and RY by RH is a physical process. This result is in agreement with these founded by Abood [26].

3.5.2. Mixed-component system (ternary system)

Mixed systems are usually present in effluent from different industries. The obtained data for mixed component systems are correlated by the four models. The parameters for each model obtained from non-linear statistical fit of the equation to the experimental data.

Table 5 represents all parameters and correlation coefficient. The adsorption isotherms for ternary

Table 4
Parameters of single-solute isotherm for RB, RR and RY onto RH

Model	Reference	Parameters	RB	RR	RY
Freundlich model $q_e = K_f C_e^{1/n}$	[24]	K_f (mg/g)(L/mg) ^{1/n}	0.803	0.384	0.173
		N	1.227	1.209	1.167
		R^2	0.996	0.987	0.990
Langmuir model $q_e = \frac{q_m b C_e}{1 + b C_e}$ $R_L = 1/(1 + b C_e)$	[25]	q_m (mg/g)	23.895	18.844	12.614
		b (L/mg)	0.029	0.016	0.011
		R^2	0.996	0.993	0.990
		R_L	0.408	0.556	0.645
Temkin model $q_e = \frac{RT}{b} \ln(K_T C_e)$	[25]	B_1 (kJ/mole)	6.360	5.831	4.137
		K_T (L/mg)	0.718	0.310	0.189
		R^2	0.973	0.993	0.987
Combination of Langmuir–Freundlich $q_e = \frac{b q_m C_e^{1/n}}{1 + b C_e^{1/n}}$	[26]	q_m (mg/g)	25.295	8.241	0.284
		b (L/mg) ^{1/n}	0.029	0.019	–0.885
		N	1.029	0.711	0.531
		R^2	0.995	0.793	0.987

Table 5
Parameters of ternary solute isotherm for RB, RR and RY onto RH

Model	Reference	Parameters	RB	RR	RY
Extended Freundlich model $q_{e,i} = \frac{K_{Fi} C_{e,i}^{ni+n1}}{C_{e,i}^{n1} + \sum_{j=1}^N K_{Fj} C_{e,j}^{nj}}$	[24]	K_f (mg/g)(L/mg) ^{1/n}	0.649	0.238	0.199
		N	1.237	1.141	1.533
		R^2	0.985	0.963	0.975
		RMSE	1.412	2.062	1.316
Langmuir model extended $q_{e,i} = \frac{q_{m,i} b_i C_{e,i}}{1 + \sum_{k=1}^N b_k C_{e,k}}$	[25]	q_m (mg/g)	19.546	12.650	4.618
		b (L/mg)	0.036	0.012	0.026
		R^2	0.997	0.976	0.976
		RMSE	0.592	2.146	2.146
Combination of Langmuir–Freundlich $q_{e,i} = \frac{q_{m,i} b_i C_{e,i}^{1/n_i}}{1 + \sum_{i=1}^N b_i C_{e,i}^{1/n_i}}$	[26]	q_m (mg/g)	8.669	4.967	5.655
		b (L/mg) ^{1/n}	0.028	0.003	0.023
		N	0.622	0.438	1.112
		R^2	0.990	0.966	0.975
		RMSE	0.673	1.996	1.316

component systems of RB, RR and RY ions onto RH are shown in Figs. 13–16.

From the above figures and Table 5 for ternary component systems, the following conclusion could be drawn:

- The extended Langmuir model seem to give the best fitting for the experimental data ($R^2=0.997, 0.976$ and 0.976) for RB, RR and RY, respectively, and this results agreed with those in the study by Sulaymon and Abood [25].
- The q_m values for the ternary systems were less than those in single systems, due to competition between the solutes.
- There is a weak competition in ternary systems in the adsorption capacity of RB ($\Delta q_{m, RB} = 4.349$ mg/g), whereas the uptake of RR and RY is reduced much more by the presence of RB solute, due to high affinity between RB and RH ($\Delta q_{m, RR} = 6.194$ and $\Delta q_{m, RY} = 7.996$ mg/g).

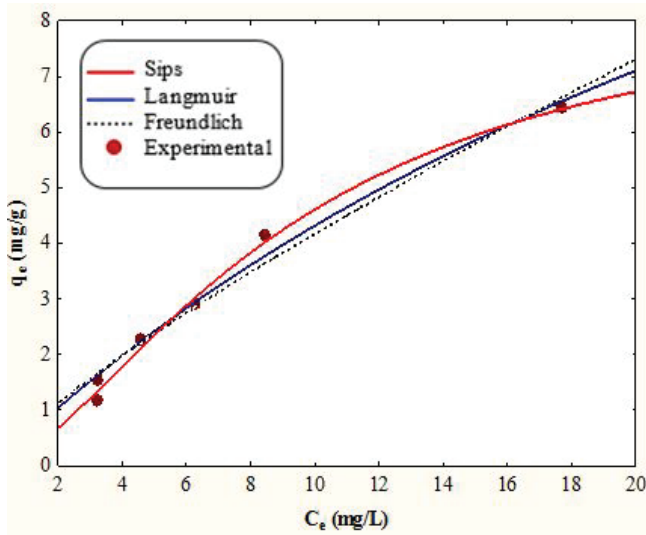


Fig. 13. Adsorption isotherm for RB onto RH in ternary system.

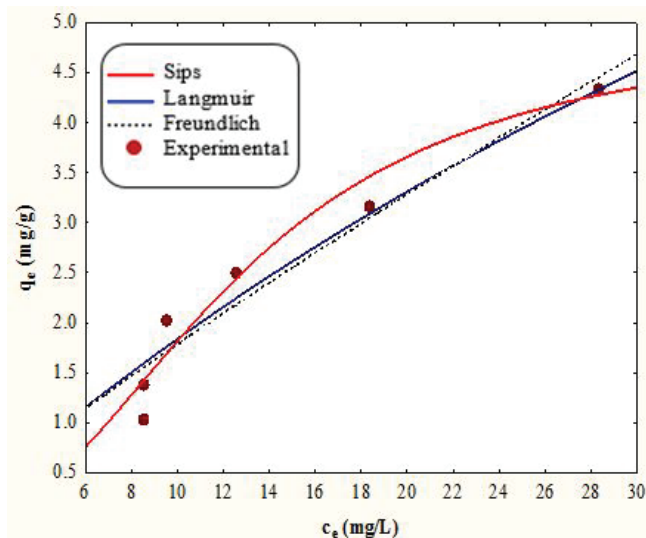


Fig. 14. Adsorption isotherm for ternary RR onto RH in ternary system.

3.6. Kinetic models

The kinetics of RB, RR and RY adsorption onto RH was analyzed using pseudo-first-order, pseudo-second-order and intra-particle diffusion kinetic models. Table 6 and Figs. 17–19 demonstrate the results of these models. The data obtained separately for each of the kinetic models from the slopes of plots show a good compliance with the pseudo-second-order equation, the correlation coefficient values for the linear plots being higher than 0.98 with adsorption uptake equal to 4.327, 3.636 and 2.644 mg/g, this is closed to the experimental uptake of 4.207, 3.566 and 2.6605 mg/g for RB, RR and RY, respectively.

The value of constant (C) in the intra-particle diffusion model is not equal to zero, suggesting that adsorption proceeds from boundary layers mass transfer across the interfaces to the intra-particle diffusion within the pores of adsorbent. This indicates that the mechanisms of dyes adsorption are complex and both the surface adsorptions as well as intra-particle diffusion contribute to the rate

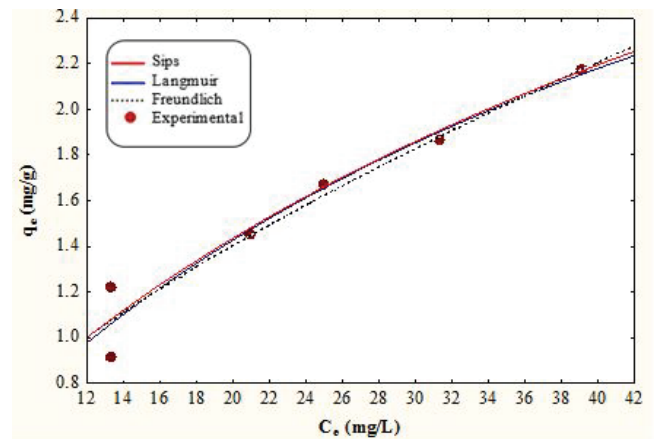


Fig. 15. Adsorption isotherm for ternary RY onto RH in ternary system.

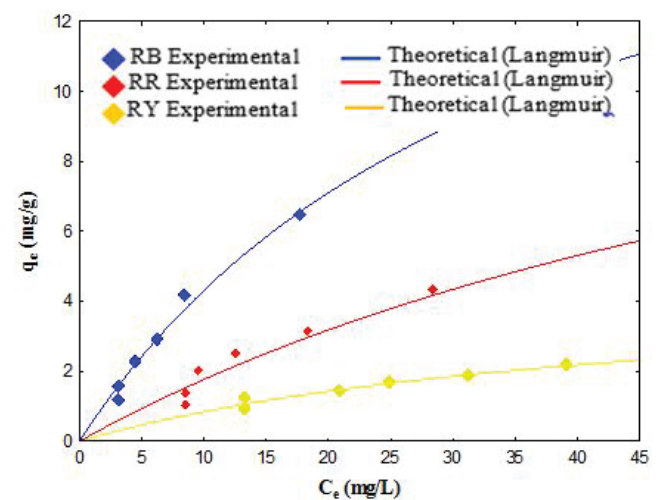


Fig. 16. RH adsorption isotherm in ternary system for RB, RR and RY using Langmuir model.

determining step and this is in agreement with those results obtained by Ong et al. [27].

3.7. FTIR analyses

Fourier transform infrared spectra (FTIR) were used to investigate the changes in vibration frequency in the functional groups of the RH due to RB, RR and RY adsorption. Each fresh and dye-loaded adsorbents were mixed separately with KBr of spectroscopic grade and made in the form of pellets at a pressure of about 1 MPa. The pellets were about 10 mm

in diameter and 1 mm thickness. Then the adsorbents were scanned in the spectral range of 4,000–400 cm⁻¹. Fig. 20 shows the FTIR spectra of RH before and after adsorption of RB, RR and RY dyes. These spectra indicated a number of absorption peaks showing the complex nature of the adsorbent. The functional group is one of the key factors to understand the mechanism of dyes binding process on natural adsorbent.

The adsorption peaks between 3,740.12 and 3,402.43 cm⁻¹ indicates the existence of free hydroxyl groups, the C–H stretching vibration around 2,985.66–2,388.34 cm⁻¹ indicates the presence of aliphatic groups. The C=C stretching

Table 6
Kinetic constants for the adsorption of RB, RR and RY onto RH

Dyes solutions	q_{exp} (mg/g)	Pseudo-first-order model				Pseudo-second order model				Intra-particle diffusion model		
		$\log(q_e - q_t) = \log(q_e) - \frac{K_L}{2.303} t$ [24]				$\frac{t}{q_t} = \frac{1}{K_2 q_e^2} + \frac{1}{q_e} t$ [25]				$q_t = K_{id} t^{1/2} + C$ [26]		
		q_{cal} (mg/g)	K_L (1/min)	R^2	RMSE	q_{cal} mg/g	K_S (g/mg min)	R^2	RMSE	K_{id} (mg/g min ^{0.5})	R^2	RMSE
RB	4.207	11.048	0.0507	0.871	2.173	4.327	0.0010	0.997	0.592	0.3976	0.836	2.196
RR	3.566	9.206	0.0449	0.899	2.065	3.636	0.0011	0.992	0.673	0.3337	0.840	2.182
RY	2.661	7.290	0.0380	0.914	2.035	2.644	0.0007	0.984	1.412	0.6322	0.949	2.021

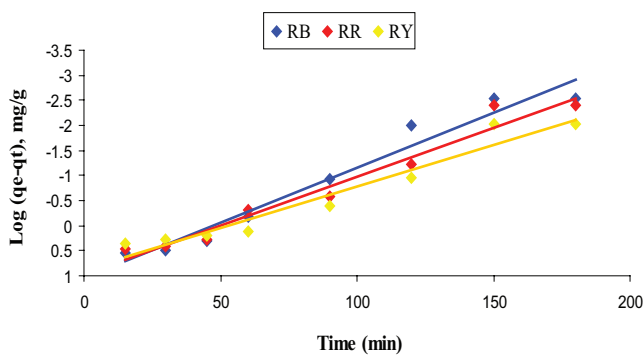


Fig. 17. Pseudo-first-order model for adsorption of RB, RR and RY onto RH.

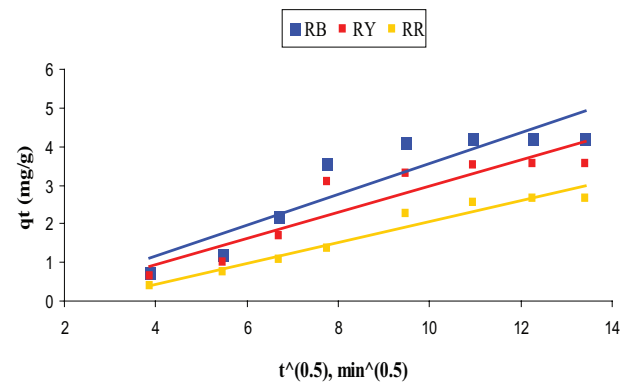


Fig. 19. Intra-particle diffusion model for adsorption of RB, RR and RY onto RH.

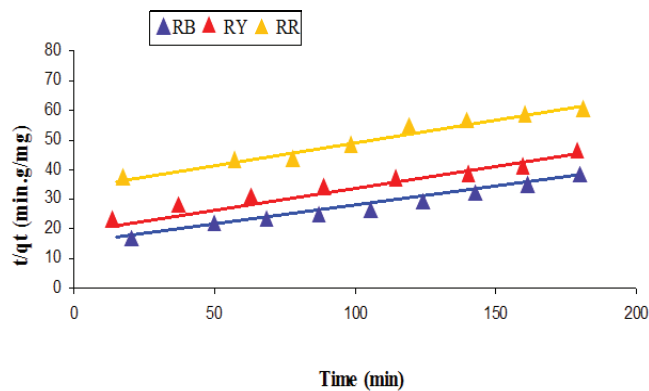


Fig. 18. Pseudo-second-order model for adsorption of RB, RR and RY onto RH.

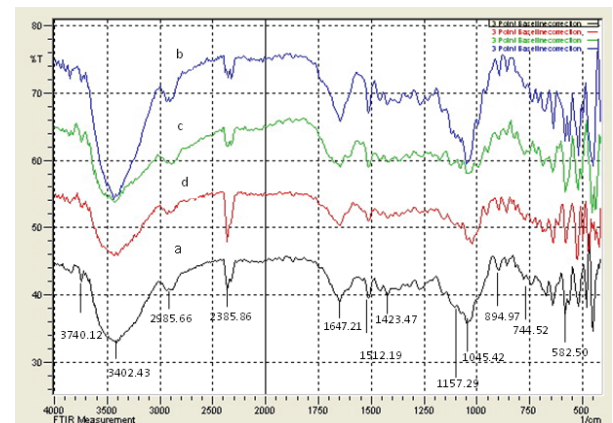


Fig. 20. FTIR spectra of (a) raw RH and (b) RB-loaded RH, (c) RR-loaded RH, (d) RY-loaded RH.

Table 7
Functional groups responsible for RB, RR and RY adsorption

Wave number, cm^{-1}	Functional groups	RB		RR		RY	
		RB-loaded RH	Δ	RR-loaded RH	Δ	RY-loaded RH	Δ
3,740.12	Surface O–H stretching	3,735.21	4.91	3,736.86	3.26	3,737.55	2.57
3,402.43	Surface O–H stretching	3,392.87	9.56	3,396.84	5.59	3,394.75	7.68
2,985.66	Aliphatic C–H stretching	2,981.34	4.32	2,982.65	3.01	2,983.87	1.79
2,388.39	Aliphatic C–H stretching	2,385.76	2.63	2,384.65	3.74	2,385.54	2.85
1,647.21	Alkene C=C Stretching	1,644.87	2.34	1,646.43	0.78	1,640.23	6.98
1,512.19	Alkene C=C stretching	1,503.65	8.54	1,505.65	6.54	1,508.98	3.21
1,423.47	P–OH stretching	1,418.65	4.82	1,420.31	3.16	1,420.99	2.48
1,157.29	Si–O stretching	1,148.43	8.86	1,150.43	6.86	1,152.74	4.55
1,045.42	Si–O stretching	1,025.76	19.66	1,035.86	9.56	1,037.75	7.67
	acid						
894.97	Si–H stretching	890.63	4.34	892.08	2.89	893.87	1.1
744.52	Si–H stretching	740.87	3.65	741.32	3.2	742.98	1.54
582.50	Si–H stretching	578.87	3.63	580.87	1.63	581.87	0.63
Summation of shifts (Δ)		$\Delta\text{RB} = 77.26$		$\Delta\text{RR} = 50.22$		$\Delta\text{RY} = 43.05$	

vibrations between 1,647.21 and 1,512.19 cm^{-1} indicative of alkenes and aromatic functional groups [28]. The peak of 1,423.47 cm^{-1} represents P–OH stretching. The peaks around 1,157.29–1,045.42 cm^{-1} and 894.97–582.50 cm^{-1} corresponds to Si–O and Si–H groups, respectively [29].

Table 7 represents the shift in the wave number of dominant peak associated with the fresh and dyes-loaded adsorbents in the FTIR plots. These shifts in the wavelength showed that there was dyes-binding process taking place at the surface of the adsorbent. There was a clear shift of wave number of hydroxyl groups –OH. The aliphatic C–H stretching also shows shift responsible for adsorption of dyes. Si–O stretching was found to have major shift of wave number so these groups play the major roles of dyes adsorption. The summation of difference in wave number before and after adsorption is 77.26, 50.22 and 50.22 cm^{-1} for RB, RR and RY, respectively. This confirms the previous results that RB had more adsorption capacity than RR and RY dyes.

4. Conclusions

In this study adsorption treatment method was applied for removing reactive dyes from simulated dye wastewater. The following conclusions were drawn:

- Prepared RH has higher removal efficiency and adsorption capacity toward reactive dyes than SS, GAC and SD adsorbents. This difference in behavior is due to the higher CEC of RH than other adsorbents.
- The maximum removal efficiency of RH depends on certain pH, dosage, contact time and initial concentration; the maximum removal efficiency is obtained at (2, 3 g, 150 min, 50 mg/L, respectively) with removal efficiency of 95.77%, 89.26% and 80.36% for RB, RR and RY, respectively.
- The equilibrium isotherm for RB, RR and RY onto RH was of favorable type, (R_L ranged from 0 to 1). In addition to the familiar Langmuir model (1918), several modern

models such as Freundlich (1907) and Temkin (1934) models were found to be in good agreement with the experimental results.

- According to Temkin model, the current adsorption process is a physical process since the heat of adsorption denoted by constant B_1 is less than 40 kJ/mole for the three reactive dyes.
- Pseudo-second-order kinetic model was found to be more suitable for adsorption of RB, RR and RY, because of higher correlation coefficients as compared with other models.
- FTIR analysis for RH showed many types of groups. However OH and Si–O groups play the important role in the adsorption of the reactive dyes from their aqueous solution. The shifts in FTIR analysis before and after adsorption for RB > RR > RY, respectively.
- The multiple correlations simulating the experimental data for adsorption processes are found to be with good fitting. The correlation coefficient R^2 is 91.581, 90.266 and 91.319 for RB, RR and RY, respectively.

The findings of this study will be used in future work to examine the tested adsorbents in continuous system using both simulated and real wastewater.

Acknowledgment

The author of the present work would like to thank Mustansiriyah University (www.uomustansiriyah.edu.iq) for its support to carry out this research.

References

- [1] Y. Miao, Biological remediation of dyes in textile effluent: a review on current treatment technologies, *Bioresour. Technol.*, 58 (2005) 217–227.
- [2] A. Ribeir, F. Graca, C. Castro, C. Vilarinho, J. Carvalho, Development of a Process for Waste Eggshell Valorisation, 4th International Conference on Engineering for Waste and Biomass Valorisation, 2012, pp. 1925–1930.

- [3] R. Guo, T. Jiao, R. Li, Y. Chen, W. Guo, L. Zhang, Q. Peng, Sandwiched Fe_3O_4 /carboxylate graphene oxide nanostructures constructed by layer-by-layer assembly for highly efficient and magnetically recyclable dye removal, *ACS Sust. Chem. Eng.*, 6 (2017) 1279–1288.
- [4] J. Carvalho, J. Araujo, F.P. Castro, Alternative low-cost adsorbent for water and wastewater decontamination derived from eggshell waste—an overview, *Waste Biomass Valorization*, 2 (2011) 157–163.
- [5] Y. Sanayei, N. Ismail, T. Teng, N. Morad, Biological treatment of reactive dye (cibacron yellow FN_2R) by sequencing batch reactor performance, *Aust. J. Basic Appl. Sci.*, 3 (2009) 4071–4077.
- [6] J.R.M. Willetts, N.J. Ashbolt, R.E. Moosbrugger, M.R. Aslam, The use of a thermophilic anaerobic system for pretreatment of textile dye wastewater, *Water Sci. Technol.*, 42 (2000) 309–316.
- [7] T. Jeric, R.J.M. Bisselink, T. Tongeren, A.M.L. Marechal, Decolorization and mineralization of reactive dyes, by the H_2O_2 /UV process with electrochemically produced H_2O_2 , *Acta Chim. Slov.*, 60 (2013) 666–672.
- [8] V.D. Balaji, D. Vinayagamoorthi, A. Palanisamy, S. Anbalagan, Degradation of reactive red HE7B and yellow FN2R dyes by fungal isolates, *J. Acad. Ind. Res.*, 1 (2012) 132–136.
- [9] B.F. Noeline, D.M. Manohar, T.S. Anirudhan, Kinetic and equilibrium modeling of lead (II) sorption from water and wastewater by polymerized banana stem in a batch reactor, *Sep. Purif. Technol.*, 45 (2005) 131–140.
- [10] I. Simkovic, J. Laszlo, Preparation of ion exchangers from bagasse by cross-linking with epichlorohydrin NH_4OH or epichlorohydrin-imidazole, *J. Appl. Polym. Sci.*, 64 (1997) 2561–2566.
- [11] M.R. Unnithan, T.S. Anirudhan, The kinetics and thermodynamics of sorption of chromium(VI) onto iron(III) complex of carboxylated polyacrylamide-grafted sawdust, *Ind. Eng. Chem. Res.*, 40 (2001) 2693–2699.
- [12] P.M. Alexander, I. Zayas, Particle size and shape effect on adsorption rate parameters, *J. Environ. Eng.*, 115 (1989) 41–55.
- [13] K. Stepova, Y. Gumnitsky, D. Maquarrie, Mechanism and mathematical model of chemisorption on modified bentonite, *J. Chem. Chem. Technol.*, 3 (2009) 169–172.
- [14] T. Papadam, P. Nikolaos, I. Poullos, Photocatalytic transformation of Acid Orange 20 and Cr (VI), *J. Photochem. Photobiol.*, 186 (2007) 308–315.
- [15] E. Ekrami, M. Okazi, Analysis of dye concentration in binary dye solution using derivative spectrophotometric techniques, *World Appl. Sci. J.*, 11 (2010) 1025–1034.
- [16] Y.S. Al-Degs, M.A. Khraisheh, S.J. Allen, M. Ahmed, G.M. Walker, Competitive adsorption of reactive dyes from solution: equilibrium isotherm studies in single and multisolite systems, *Chem. Eng. J.*, 128 (2007) 163–167.
- [17] Y. AL-Degs, A.H. El-Sheikh, M.A. Al-Gouti, M.S. Sunjuk, Determination of commercial colorants in different water bodies using partial least squares regression(PLS), *Jord. J. Chem.*, 3 (2008) 321–336.
- [18] Q. Kang, Residual color profiles of simulated reactive dyes wastewater in flocculation, *J. Sep. Purif. Technol.*, 57 (2007) 356–365.
- [19] P.L. De-Alba, L.L. Martinze, L.I. Rodriguez, J.A. Hernandez, Extraction of sunset yellow and tartrazine and determination by bivariate calibration and derivative spectrophotometry, *Analyst*, 122 (1997) 1575–1579.
- [20] A. Shukla, Y.H. Zhang, P. Dubey, J.L. Margrave, S.S. Shukla, The role of saw dust in the removal of unwanted materials from water, *J. Hazard. Mater.*, 95 (2002) 137–152.
- [21] A. Ahmadpour, D.D. Do, The preparation of activated carbon by chemical activation, *Carbon*, 35 (1997) 1723–1732.
- [22] N.J. Ara, M.A. Hasan, M.R. Rahman, M.A. Salam, A. Salam, A.M.S. Alam, Removal of remazol red from textile waste water using treated sawdust – an effective way of effluent treatment, *Bangladesh Pharm. J.*, 16 (2013) 93–98.
- [23] L.J. Yu, S.S. Shukla, K.L. Dorris, A. Shukla, J.L. Margrave, Adsorption of chromium from aqueous solutions by Maple sawdust, *J. Hazard. Mater.*, 100 (2003) 53–63.
- [24] E. Alver, A.E.U. Metin, Anionic dye removal from aqueous solutions using modified zeolite: adsorption kinetics and isotherm studies, *Chem. Eng. J.*, 200 (2012) 59–67.
- [25] A.H. Sulaymon, W.M. Abood, Competitive adsorption of three reactive dyes by activated carbon, *J. Eng.*, 19 (2013) 656–667.
- [26] W.M. Abood, Removal of Three Textile Reactive Dyes (Blue, Red and Yellow) by Activated Carbon and Low-cost Adsorbents, Ph.D. Thesis University of Baghdad, College of Engineering, 2012.
- [27] S. Ong, W. Lee, P. Keng, S.T. Ha, Equilibrium studies and kinetic mechanism for the removal basic and reactive dyes in both single and binary system using EDTA modified rice husk, *Int. J. Phys. Sci.*, 5 (2010) 582–595.
- [28] I.D. Mall, V.C. Srivastavan, I.M. Mishre, Characterization of mesoporous rice husk ash (RHA) and adsorption kinetics of metal ions from aqueous solution onto RHA, *J. Hazard. Mater. B*, 134 (2006) 257–267.
- [29] Y. Safa, H.N. Bhatti, Adsorptive removal of direct dyes by low cost rice husk, *Afr. J. Biotechnol.*, 10 (2011) 3128–3142.